THE JOURNAL OF BIOLOGICAL CHEMISTRY
Vol. 278, No. 45, Issue of November 7, pp. 44331–44337, 2003
Printed in U.S.A.

ATPase and DNA Helicase Activities of the *Saccharomyces cerevisiae* Anti-recombinase Srs2*

Received for publication, July 7, 2003, and in revised form, September 2, 2003
Published, JBC Papers in Press, September 8, 2003, DOI 10.1074/jbc.M307256200

Stephen Van Komen‡§¶, Mothe Sreedhar Reddy‡§‖, Lumir Krejci‡¶, Hannah Klein, and Patrick Sung¶‡‡**

*From the ‡Institute of Biotechnology and Department of Molecular Medicine, University of Texas Health Science Center, San Antonio, Texas 78245 and **Department of Biochemistry and Kaplan Comprehensive Cancer Center, New York University School of Medicine, New York, New York 10016*

Saccharomyces cerevisiae SRS2 **encodes an ATP-dependent DNA helicase that is needed for DNA damage checkpoint responses and that modulates the efficiency of homologous recombination. Interestingly, strains simultaneously mutated for *SRS2* and a variety of DNA repair genes show low viability that can be overcome by inactivating homologous recombination, thus implicating inappropriate recombination as the cause of growth impairment in these mutants. Here, we report on our biochemical characterization of the ATPase and DNA helicase activities of Srs2. ATP hydrolysis by Srs2 occurs efficiently only in the presence of DNA, with ssDNA being considerably more effective than dsDNA in this regard. Using homopolymeric substrates, the minimal DNA length for activating ATP hydrolysis is found to be 5 nucleotides, but a length of 10 nucleotides is needed for maximal activation. In its helicase action, Srs2 prefers substrates with a 3′ ss overhang, and ~10 bases of 3′ overhanging DNA is needed for efficient targeting of Srs2 to the substrate. Even though a 3′ overhang serves to target Srs2, under optimized conditions blunt-end DNA substrates are also dissociated by this protein. The ability of Srs2 to unwind helicase substrates with a long duplex region is enhanced by the inclusion of the single-strand DNA-binding factor replication protein A.**

DNA helicases are ubiquitous among prokaryotes and eukaryotes. These enzymes utilize the free energy derived from the hydrolysis of a nucleoside triphosphate to disrupt the hydrogen bonds that bind the complementary strands of duplex DNA. DNA helicases play an essential role in virtually every aspect of nucleic acid metabolism, including transcription, replication, recombination, and repair (reviewed in 1–3).

We focus on the mechanism of homologous recombination in eukaryotes and are interested in the biology of DNA helicases that influence recombination events. One such helicase is encoded by the *Saccharomyces cerevisiae SRS2*[1] (*S*uppressor of *R*AD *S*ix-screen mutant *2*) gene. Srs2 protein belongs to the SF1 helicase family and contains regions of similarity to the bacterial UvrD, Rep, and PcrA helicases (4). A mutant form of *SRS2* was initially identified as a suppressor of the radiation-sensitivity of *rad6* and *rad18* mutants that are defective in post-replicative DNA repair (4, 5). Subsequent studies revealed that suppression of *rad6* and *rad18* mutations by the *srs2* mutation is due to heightened recombination mediated by the *RAD52* epistasis group of genes (6). Consistent with this observation, *srs2* mutants show a hyper-recombination phenotype (7, 8). Together, these genetic observations indicate that *SRS2* negatively regulates *RAD52*-mediated homologous recombination. It has been suggested that by antagonizing the recombination machinery, Srs2 ensures the channelling of DNA lesions that arise during DNA replication into the Rad6/Rad18-mediated repair reactions (4). Hence, in *rad6* and *rad18* mutants, repair of the replication-associated DNA lesions by recombination is inefficient unless *SRS2* is inactivated (4).

Multiple studies have shown that inactivating *SRS2* in cells already mutated for one of a number of genes needed for DNA metabolism results in poor growth and sometimes inviability (6, 9–11). Interestingly, simultaneous ablation of homologous recombination (*i.e.* by deleting *RAD51, RAD52, RAD55*, and *RAD57*, members of the *RAD52* epistasis group) restores viability to the double mutants, implicating inappropriate recombination as the underlying cause of growth impediment in these mutants (11–13). In some instances (*i.e. srs2*Δ *rad54*Δ and *srs2*Δ *rdh54*Δ), cell inviability can also be overcome by deleting genes that function in DNA damage checkpoints, which suggests that growth impairment is caused by the formation of a recombination intermediate that is sensed by DNA damage checkpoints to result in prolonged cell cycle arrest and eventual cell death (13). Srs2 protein has also been implicated in signaling events in the intra-S checkpoint in cells treated with a DNA damaging agent (13, 14). More recently, a role for Srs2 in mediating adaptation and recovery from DNA damage checkpoint-imposed G_2/M arrest has been reported (15). Deletion of *RAD51* enables *srs2*-null cells to recover from DNA damage checkpoint-mediated cell cycle arrest (15), implicating Rad51 in the prevention of recovery in the *srs2* mutant.

The involvement of the *SRS2* gene in the modulation of recombination and DNA damage checkpoint responses, which have a direct bearing on the maintenance of genome integrity,

* This work was supported by United States Public Health Service Research Grants ES07061, CA96593, GM53738, and GM57814. The costs of publication of this article were defrayed in part by the payment of page charges. This article must therefore be hereby marked "*advertisement*" in accordance with 18 U.S.C. Section 1734 solely to indicate this fact.

§ These authors contributed equally to this work.
¶ Present address: Dept. of Molecular Biophysics and Biochemistry, Yale University School of Medicine, 333 Cedar St., C130 Sterling Hall of Medicine, New Haven, CT 06520-8024.
‖ Present address: Dept. of Pathology, Brigham and Women's Hospital and Harvard Medical School, 75 Francis St., Boston, MA 02115.
‡‡ To whom correspondence should be addressed: Dept. of Molecular Biophysics and Biochemistry, Yale University School of Medicine, 333 Cedar St., C130 Sterling Hall of Medicine, New Haven, CT 06520-8024. Tel.: 203-785-4553; Fax: 203-785-6404; E-mail: Patrick.Sung@yale.edu.

[1] The abbreviations used are: *SRS2*, suppressor of RAD six-screen mutant 2 gene; RPA, replication protein A; ss, single strand; AMP-PNP, adenosine 5′-(β,γ-imino)triphosphate; AMP-PCP, adenosine 5′-(β,γ-methylene)triphosphate; ATPγS, adenosine 5′-3-*O*-(thio)triphosphate.

TABLE I
Oligonucleotides used

Name of the oligonucleotide	DNA sequence (5′ to 3′)
H1	ATTAAGCTCTAAGCCATGAA TTCAAATGAC CTCTTATCAA
H2	TTGATAAGAG GTCATTTGAA TTCATGGCTT AGAGCTTAAT
H3	TTGATAAGAG GTCATTTGAA TTCATGGCTT AGAGCTTAAT TGCTGAATCT GGTGCTGGGA TCCAACATGT TTTAAATATG
H4	ATGTCACTAT TGAAGCGCTG ATCACTGTCT CCATCGAACG TTGATAAGAG GTCATTTGAA TTCATGGCTT AGAGCTTAAT
H5	ATTAAGCTCTAAGCCATGAA TTCAAATGAC CTCTTATCAA ATCTGATGCT ATAGGCTAGC
H6	TTGATAAGAG GTCATTTGAA TTCATGGCTT AGAGCTTAAT AGTCGTATTA ATGCTATGAT
H7	GCTTAGTCAT GTCAGTATAT ATTAAGCTCTAAGCCATGAA TTCAAATGAC CTCTTATCAA
H8	ATGTCACTGT CGCTATGTAT TTGATAAGAG GTCATTTGAA TTCATGGCTT AGAGCTTAAT
H9	TTGATAAGAG GTCATTTGAA TTCATGGCTT AGAGCTTAA TT
H10	TTGATAAGAG GTCATTTGAA TTCATGGCTT AGAGCTTAA TTTTTT
H11	TTGATAAGAG GTCATTTGAA TTCATGGCTT AGAGCTTAA TTTTTTTTT
H12	TTGATAAGAG GTCATTTGAA TTCATGGCTT AGAGCTTAA TTTTTTTTTTT
H13	TTGATAAGAG GTCATTTGAA TTCATGGCTT AGAGCTTAA TTTTTTTTTTTTT
H14	TTGATAAGAG GTCATTTGAA TTCATGGCTT AGAGCTTAA TTTTTTTTTTT TTTTTT
P1	GAGTTTTATCGCTTCCATGACGCAGAAG
P2	TTTCTCATTTTCCGCCAGCAGTCCACTTCG
P3	CAGAAAATCGAAATCATCTTCGGTTAAATC

underscores the importance for biochemical characterization of its encoded product. Previously, a recombinant form of Srs2 tagged with a C-terminal six-histidine sequence was expressed in *Escherichia coli* but was found to be insoluble. Nonetheless, the histidine-tagged Srs2 protein could be extracted from the inclusion bodies with 6 M guanidine and enriched by passing the solubilized fraction over a nickel-NTA column and eluting the bound proteins under denaturing conditions. Following gel filtration, a renaturation protocol was used to obtain a small amount of soluble Srs2 protein. The renatured Srs2 protein was shown to possess a modest ssDNA-dependent ATPase activity and also a DNA helicase activity that has a 3′ to 5′ polarity with respect to the ssDNA on which the protein translocates (16). To define the biochemical properties of Srs2, we have achieved expression of soluble Srs2 in *E. coli* and have devised a procedure that entails conventional chromatographic fraction steps for its purification. Here we show that the non-tagged, soluble Srs2 has a robust ssDNA-dependent ATPase activity. We also carry out a more detailed characterization of the DNA helicase activity of Srs2 and study its functional interaction with the single-strand binding factor replication protein A (RPA) in DNA unwinding.

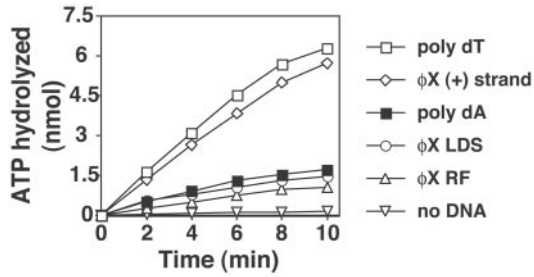

FIG. 1. **DNA-dependent ATPase activity of Srs2.** Reactions containing 35 nM Srs2, 1.5 mM [γ-^{32}P]ATP, and one of a number of DNA cofactors (25 μM nucleotides each) were incubated at 30 °C and pH 7.6 in the presence of 15 mM KCl. The level of ATP hydrolysis was measured by thin layer chromatography and phosphorimaging analysis. The DNA co-factors were ϕX viral (+) strand, ϕX linear duplex DNA designated as ϕX LDS, ϕX replicative form I DNA (~90% supercoiled) designated as ϕX RF, poly(dA), and poly(dT). The averaged values from three independent experiments were plotted.

MATERIALS AND METHODS

Srs2 Expression and Purification—The plasmid pET11c::Srs2 containing the *SRS2* gene under the control of the isopropyl-β-D-thiogalactopyranoside-inducible T7 promoter (17) was introduced into *E. coli* BL21(DE3). Overnight cultures grown in Luria broth at 37 °C were diluted 500-fold into fresh medium and incubated at 37 °C until the OD_{600} reached 1.2. At that time, isopropyl-β-D-thiogalactopyranoside was added to 0.1 mM, and the culture was incubated at 16 °C for 24 h. Cells were harvested by centrifugation and stored at −80 °C. All the subsequent steps were carried out at 0–4 °C. Extract was prepared by using a French press from 150 g of cell paste (obtained from 70 liters of culture) in 450 ml of cell breakage buffer (50 mM Tris-HCl, pH 7.5, 600 mM KCl, 10% sucrose, 5 mM EDTA, 2 mM dithiothreitol, and the following protease inhibitors: aprotinin, chymostatin, leupeptin, and pepstatin A, each at 5 μg/ml). The extract was clarified by ultracentrifugation (100,000 × *g* for 90 min) and treated with ammonium sulfate (0.21 g/ml) to precipitate Srs2 and about 15% of the total protein. The precipitated proteins were harvested by centrifugation and then dissolved in 400 ml of T buffer (40 mM Tris-HCl, pH 7.5, 10% glycerol, 0.01% Igepal (Sigma), 1 mM dithiothreitol, and the aforementioned protease inhibitors) to yield a protein solution (fraction I) that had conductivity equivalent to 150 mM KCl. This protein solution was passed through a 90-ml column of Q-Sepharose, and the flow through fraction from the Q column (fraction II) was applied onto a 70-ml SP-Sepharose column, which was developed with a 900 ml gradient of 120 to 500 mM KCl in T buffer. As identified by immunoblotting and staining of SDS-polyacrylamide gels with Coomassie Blue, Srs2 eluted from the SP column at ~350 mM KCl; the pool (fraction III, total = 100 ml) was fractionated in a 6-ml column of macro-hydroxyapatite (Bio-Rad) using a 90-ml gradient of 60–340 mM KH_2PO_4 in T buffer. Srs2 eluted from the hydroxyapatite column at ~220 mM KH_2PO_4, and the peak fractions were pooled (fraction IV, total = 14 ml) and dialyzed against T buffer for 90 min to lower the conductivity to that of 60 mM KCl. The dialysate was fractionated in a 1-ml Mono Q column with a 30 ml, 50–200 mM KCl gradient in T buffer, with Srs2 eluting at ~120 mM KCl. The pool of Srs2 from the Mono Q column (fraction V, total = 2 ml) was diluted with 3 ml of buffer T and then re-fractionated in Mono Q using the same gradient. The final Srs2 pool (fraction VI, total = 2 ml containing 300 μg of Srs2) was concentrated to 150 μl in a Centricon-30 device (Amicon) and stored in 2-μl portions at −80 °C.

RPA—RPA was purified from a bacterial strain tailored to co-express the three subunits of this factor (18) using our published protocol (19).

DNA Substrates, Helicase Substrates, and Oligonucleotides—The ϕX174 viral (+) strand was purchased from New England Biolabs. The ϕX174 replicative form I DNA (~90% supercoiled form; Invitrogen) was linearized by digestion with ApaL I. The oligonucleotides used for this study were purchased from Invitrogen and are listed in Table I. H1, H5, and H6 were 5′-end-labeled with [γ^{32}-P]ATP using T4 polynucleotide kinase. The unincorporated isotope was removed by passing the substrates through a Spin30 column (Bio-Rad). Oligonucleotides H1 and H2 were annealed to create a 40-base pair blunt-end DNA duplex. This 40-base pair duplex region was retained in the other helicase substrates. Oligonucleotides H1 and H3 were hybridized to each other to obtain a partial duplex with a 40-nucleotide ssDNA overhang at the 3′ end. To obtain a partial duplex with a 40-nucleotide ssDNA overhang at the 5′ end, oligonucleotides H1 and H4 were annealed to each other. Oligonucleotides H5 with H6 were annealed to each other to give a substrate that possessed two 3′ overhangs of 20 nucleotides each, and oligonucleotide H7 was hybridized with H8 to yield a substrate that had two 5′ overhangs of 20 nucleotides each. The substrates with 3′-poly(dT) overhangs of 2, 5, 8, 10, 12, and 16 nucleotides were prepared by annealing oligonucleotide H1 to H9, H10, H11, H12, H13, and H14,

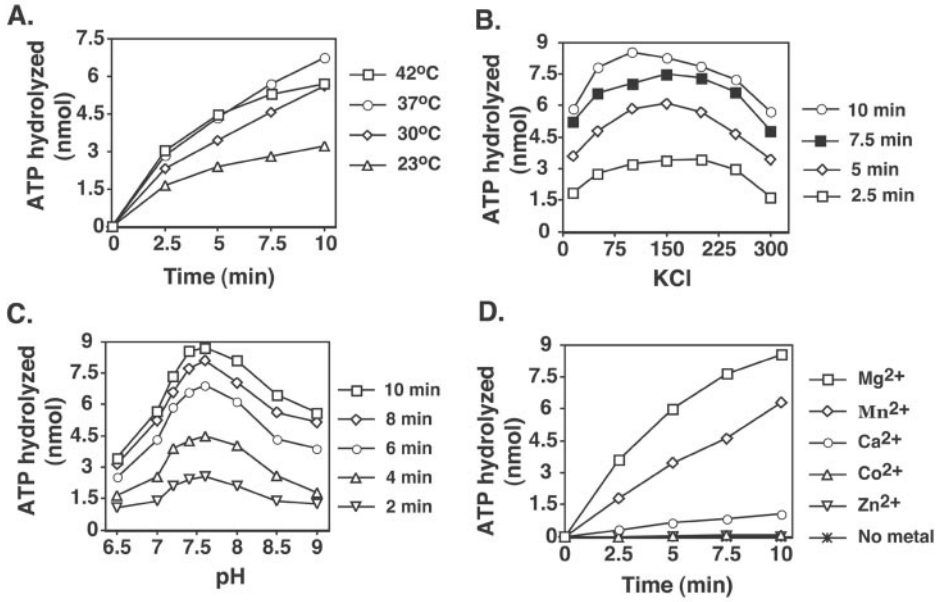

FIG. 2. **Reaction parameters that affect the efficiency of ATP hydrolysis.** *A*, ATPase reactions were assembled with 35 nM Srs2, 1.5 mM [γ-^{32}P]ATP, 2.5 mM Mg^{2+}, and ϕX174 viral (+) strand (25 μM nucleotides) in pH 7.6 buffer that contained 15 mM KCl and were incubated at 23 °C, 30 °C, 37 °C, and 42 °C. *B*, ATPase reactions were carried out at 30 °C in the presence of 15, 50, 100, 150, 200, 250, and 300 mM KCl as in *A*. *C*, ATPase reactions were carried out at 30 °C in buffers with pH of 7.0, 7.2, 7.4, 7.6, 8, 8.5, and 9.0 and containing 100 mM KCl as in *A*. *D*, ATPase reactions were carried out at 30 °C in pH 7.6 buffer that contained 100 mM KCl as in *A*, except that Mg^{2+} was either omitted or substituted with 2.5 mM of Mn^{2+}, Ca^{2+}, Co^{2+}, and Zn^{2+}. In *A–D*, the averaged values from at least two independent experiments were plotted.

respectively. Annealing reactions were carried out by heating equimolar amounts of the indicated oligonucleotides at 95 °C for 10 min in buffer B (50 mM Tris-HCl, pH 7.5, 10 mM $MgCl_2$, and 100 mM NaCl), followed by slow cooling to room temperature. The annealed DNA substrates were separated from the unhybridized oligonucleotides in 12% polyacrylamide gels run in TAE buffer (40 mM Tris acetate, pH 7.4, 0.5 mM EDTA), and the substrates were recovered from the gel as described (20). For the construction of the ϕX174-based helicase substrates, two fragments of 150 of 500 bp were amplified by PCR in the presence of [α-^{32}P]dATP using primer pairs P1/P2 and P1/P3 and ϕX174 RF DNA as template. The PCR-amplified ^{32}P-labeled DNA fragments were purified and hybridized to ϕX174 (+) strand, and the resulting substrates were purified, as described (21).

ATPase Assay—Unless stated otherwise, Srs2 (35 nM) was mixed with the DNA cofactor (25 μM nucleotides) in 10 μl of buffer A (30 mM Tris-HCl, pH 7.6, 2.5 mM $MgCl_2$, 1 mM dithiothreitol, and 100 μg/ml bovine serum albumin) containing 1.5 mM [γ-^{32}P]ATP and the indicated amounts of KCl. The reactions were incubated at the indicated temperatures, and 2-μl aliquots were removed at the indicated times and mixed with an equal volume of 500 mM EDTA. The released phosphate was separated from the unhydrolyzed ATP by thin layer chromatography, as described (20). The levels of $^{32}P_i$ and [γ-^{32}P]ATP in the reactions were determined by phosphorimaging analysis of the thin layer chromatography plates in a Personal Molecular Imager FX (Bio-Rad). To determine the reaction background, a reaction mixture without Srs2 was incubated as above, and the amount of $^{32}P_i$ was determined and subtracted from the values obtained with Srs2 present. The buffers with pH 7.0–9.0 in Fig. 2*C* were based on 30 mM Tris-HCl.

In the experiment presented in *panel II* of Fig. 4*B*, the indicated amounts of ATP, ADP, AMP-PCP, AMP-PNP, and ATPγS were mixed with 7 nM Srs2 in 10 μl of buffer A containing 0.1 mM [γ-^{32}P]ATP and 125 mM KCl. The reactions were incubated at 23 °C for 3 min and then analyzed as above.

DNA Helicase Assay—Unless stated otherwise, Srs2 was incubated at 30 °C with the helicase substrates (150 nM nucleotides) in 10 μl of buffer H (30 mM Tris-HCl, pH 7.6, 2.5 mM $MgCl_2$, 2 mM ATP, 100 mM KCl, 1 mM dithiothreitol, and 100 μg/ml bovine serum albumin) containing an ATP-regenerating system consisting of 20 mM creatine phosphate and 20 μg/ml creatine kinase. Aliquots of the reactions were drawn at the indicated times and treated with SDS (0.2% final) and proteinase K (0.5 mg/ml) at 37 °C for 3 min. The released ^{32}P-labeled DNA fragment was separated from the unreacted substrate in 12 or 15% nondenaturing polyacrylamide gels in TAE buffer (40 mM Tris acetate, pH 7.4, containing 0.5 mM EDTA) at 4 °C, as described (20). Gels were dried onto Whatman DE81 paper and then analyzed in the PhosphorImager. The ϕX174-based substrates were incubated with Srs2 as above. When present, RPA was added with Srs2 to the DNA substrates. After deproteinization treatment, the reactions were analyzed in 1.5% agarose gels in TAE buffer at 4 °C. The agarose gels were dried and analyzed as above. When comparing the ϕX174-based substrates with 150- and 500-bp duplex regions, the reaction mixtures were resolved on a 6% nondenaturing polyacrylamide gel in TAE buffer at 4 °C. The gel was dried and analyzed as above.

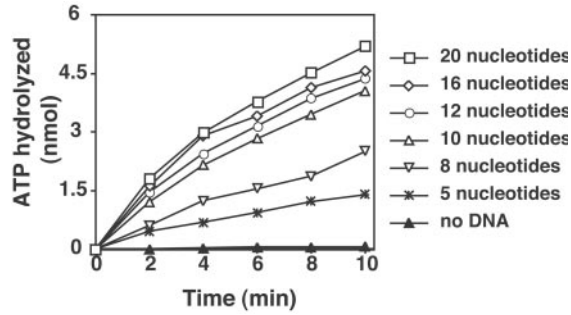

FIG. 3. **Relationship between ssDNA length and ATP hydrolysis.** ATPase reactions containing 15 mM KCl were assembled and incubated at 30 °C as described in Fig. 1*A*, except that dT oligomers of 5, 8, 10, 12, 14, 16, and 20 nucleotides were used as the DNA co-factors. The averaged values from two independent experiments were plotted.

RESULTS

Srs2 Protein Purification—We have recently described the expression of Srs2 that does not contain an affinity tag in *E. coli* (17). Although cells grown at 37 °C yield predominantly insoluble Srs2, the solubility of this protein is greatly improved upon decreasing the growth temperature to 16 °C. The soluble Srs2 was purified to near homogeneity using a six-step procedure including ammonium sulfate precipitation and chromatographic fractionation through Q-Sepharose, SP-Sepharose, Macro-hydroxyapatite, and Mono Q columns, as described under "Materials and Methods." The final protein pool from the Mono Q step was greater than 95% homogeneous (17).

DNA-dependent ATPase Activity of Srs2—We examined the purified Srs2 protein for ATPase activity in the absence of DNA and with the viral (+) strand or the replicative form of ϕX174 phage. The amount of ATP hydrolysis was monitored by thin layer chromatography, as we had done before (20). As summarized in Fig. 1, while little ATPase was seen in the absence of DNA (*inverted triangles*), addition of either viral (+) strand (*diamonds*) or the replicative form DNA (*triangles*) led to efficient ATP hydrolysis, with the former being much more effective in ATPase activation. Interestingly, although the homopolymer poly(dT) (*white squares*) was as effective as the ϕX

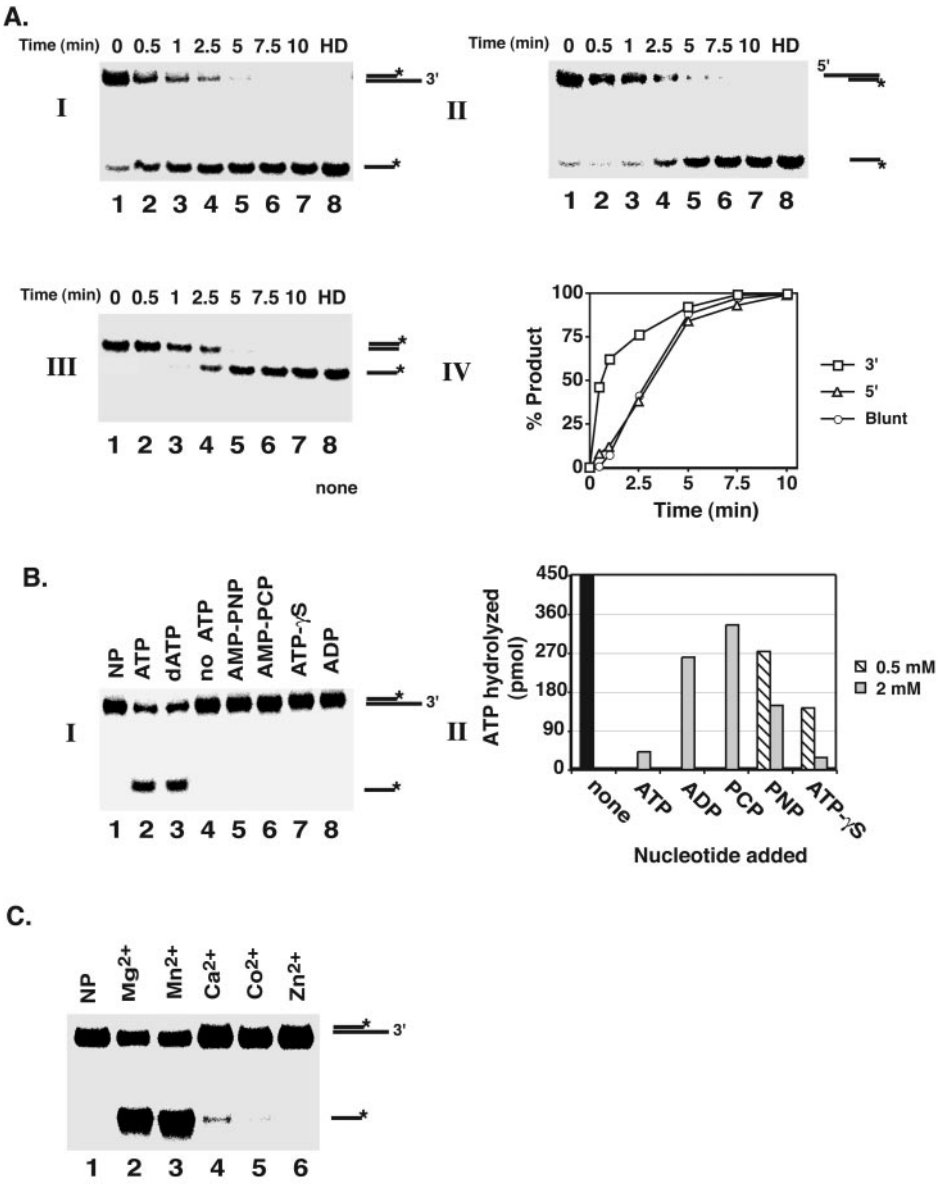

FIG. 4. **DNA helicase activity of Srs2.** *A*, Srs2 (30 nM) was incubated at 30 °C for the indicated times with 40-bp DNA helicase substrates (150 nM nucleotides each) that contained a 3′ 40-nucleotide overhang (*panel I*), a 5′ 40-nucleotide overhang (*panel II*), or no ss overhang (*panel III*). In *lane 8* of all three panels, the substrate was boiled for 1 min (*HD*) to release the hybridized ^{32}P-labeled oligonucleotide. The results from *panels I*, *II*, and *III* are plotted in *panel IV*. All the experiments were repeated at least twice with very similar results. *, position of the ^{32}P label. *B*, *I*, the 3′ substrate (300 nM nucleotides) was incubated at 23 °C for 5 min with Srs2 (20 nM) in buffer with ATP (*lane 2*), dATP (*lane 3*), AMP-PMP (*lane 5*), AMP-PCP (*lane 6*), ATPγS (*lane 7*), ADP (*lane 8*), or without any nucleotide (*lane 4*). In *lane 1*, the substrate was incubated in the ATP-containing buffer without Srs2 (*NP*). *, the position of the ^{32}P label. *II*, Srs2 (7 nM) was incubated for 3 min at 23 °C with ATP (0.1 mM [γ-^{32}P]ATP), ssDNA (30 μM), and the indicated amounts of unlabeled ATP, ADP, AMP-PCP, AMP-PNP, and ATPγS. The hydrolysis of the labeled ATP was quantified as described under "Materials and Methods." The averaged values from two independent experiments were plotted. *C*, the 3′ substrate (300 nM nucleotides) was incubated at 23 °C for 5 min with Srs2 (20 nM) in the ATP-containing buffer with Mg^{2+} (*lane 2*), Mn^{2+} (*lane 3*), Ca^{2+} (*lane 4*), Co^{2+} (*lane 5*), and Zn^{2+} (*lane 6*). *Lane 1*, the substrate was incubated in the ATP-containing buffer with Mg^{2+} but no Srs2 (*NP*). *, the position of the ^{32}P label.

viral (+) in activating ATP hydrolysis, poly(dA) (*black squares*) was a poor cofactor.

The optimal reaction temperature for ATP hydrolysis by Srs2 was found to be 37 °C. At 42 °C, the rate of ATP hydrolysis started declining after a few minutes of incubation, probably because of thermal denaturation of Srs2 protein (Fig. 2*A*). As shown in Fig. 2*B*, the activity of Srs2 was stimulated by 50–250 mM of KCl, with significant inhibition occurring at 300 mM of the salt. The optimal pH range was determined to be 7.25–8.0 (Fig. 2*C*), and a dependence on Mg^{2+} was noted (Fig. 2*D*). Although Mn^{2+} was nearly as effective as Mg^{2+} in ATPase activation, little or no ATP hydrolysis was seen with Ca^{2+}, Co^{2+}, or Zn^{2+} (Fig. 2*D*).

The ATPase activity Srs2 is rather robust. For instance, Srs2 exhibited a kcat for ATP hydrolysis ≥ 3000 min^{-1} at 37 °C, measured with ϕX viral (+) strand as cofactor (Fig. 2*C*). Rong and Klein (16) previously reported that renatured Srs2 protein had a kcat for ATP hydrolysis of ~191 min^{-1} with M13mp18 viral (+) strand as cofactor (16). Because we know that M13 viral (+) strand is just as effective as ϕX viral (+) strand in ATPase activation (data not shown), the Srs2 protein that we have prepared is significantly more active in ATP hydrolysis.

Minimal Length of DNA Required for ATPase Activation—Next we investigated the minimal length of ssDNA needed for activating the Srs2 ATPase activity. For this purpose, homopolymeric dT oligomers that were 5, 8, 10, 12, 14, 16, and 20 nucleotides in length were used as cofactors in the ATPase reaction. A low level of ATP hydrolysis was seen with the 5-mer and 8-mer substrates (Fig. 3). Increasing the length of the DNA to 10 nucleotides resulted in a large increase in ATP hydrolysis, but the substrates with lengths of 16 and 20 nucleotides gave only incremental elevation in hydrolysis rate over the 10-mer substrate. These results indicate that the effective site size for the activation of the Srs2 ATPase function is ~10 nucleotides.

DNA Helicase Activity of Srs2—To characterize the DNA unwinding activity of Srs2, we used three different ^{32}P-labeled DNA substrates (Fig. 4) that shared an identical 40-base pair duplex region but differed from one another in possessing a 40-base 3′ tail (3′ substrate), a 40-base 5′ tail (5′ substrate), or no ss tail (blunt substrate). Displacement of the ^{32}P-labeled oligonucleotide was monitored by electrophoresis in polyacrylamide gels and quantified by phosphorimaging analysis of the dried gels. We used a reaction temperature of 30 °C for this experiment. As shown in Fig. 4*A*, after only 1 min of incubation, the majority (>60%) of the 3′ substrate had been unwound by Srs2 (Fig. 4*A*, *panel I*, *lane 3*). At this time, little of the 5′

substrate (Fig. 4A, *panel II*, *lane 3*) or blunt substrate (Fig. 4*A*, *panel III*, *lane 3*) had been unwound. However, significant unwinding of the 5′ substrate and blunt substrate was seen after 2.5 min of incubation, with >50% dissociation of these two substrates at 5 min (Fig. 4*A*, *panels II* and *III*, *lane 5*). Our data indicate that Srs2 prefers to act on the substrate with the 3′ ss overhang, which is consistent with the 3′ to 5′ polarity seen by Rong and Klein (16), and they additionally reveal that Srs2 can unwind substrates without such an overhang. As shown in Fig. 4*B*, *panel I*, no unwinding was seen upon the omission of ATP or substitution of ATP with AMP-PNP, AMP-PCP, ATPγS, or ADP. To determine whether the failure of Srs2 to unwind DNA (Fig. 4*B*, *panel I*) was caused by an inability to bind the latter nucleotides, ATPase assays were performed with the addition of AMP-PNP, AMP-PCP, ATPγS, or ADP as potential inhibitors. As shown in Fig. 4*B*, *panel II*, the amount of ^{32}P-labeled ATP hydrolyzed by Srs2 was reduced by all these nucleotides, with the most pronounced inhibition seen with the addition of ATPγS. Thus, these results provide supporting evidence that ATP hydrolysis by Srs2 is needed for DNA unwinding. In addition, DNA unwinding occurred in the presence of Mg^{2+} or Mn^{2+}, but little or no DNA unwinding activity was seen when Ca^{2+}, Co^{2+}, or Zn^{2+} was used (Fig. 4*C*).

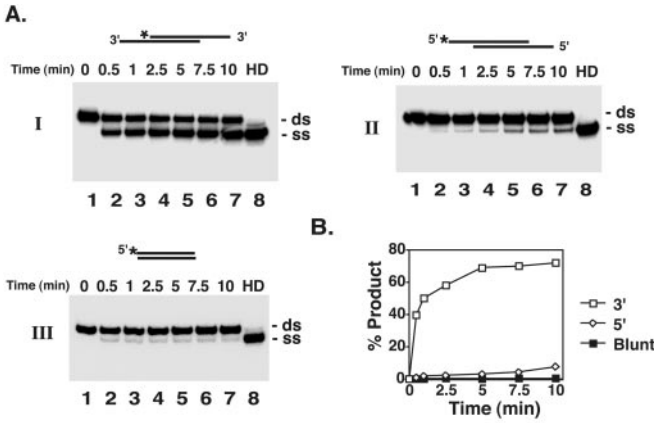

FIG. 5. **Preferential unwinding of substrates with 3′ ss overhangs.** *A*, Srs2 (20 nM) was incubated for the indicated times at 23 °C with 40-bp DNA substrates (300 nM nucleotides) that contained 20-nucleotide 3′ (*panel I*) or 5′ (*panel II*) ss overhangs at both ends or blunt ends (*panel III*). In *lane 8* of each panel, the helicase substrate was boiled for 1 min (*HD*) to release the radiolabeled fragment. *, the position of the ^{32}P label. *B*, the results from *panels I*, *II*, and *III* were plotted. *ds*, double strand. All the experiments were repeated twice with very similar results.

A 5′ Overhang Is Ineffective in Srs2 Recruitment—The results presented above indicate that in its DNA helicase action, Srs2 prefers the substrate with a 40-nucleotide 3′ ss tail but can also unwind the substrates with either a 40-nucleotide 5′ overhang or without any overhang. We wished to further examine whether a 5′ overhang confers an advantage in terms of Srs2 recruitment. To address this question, we constructed another set of substrates that had a 3′ tail at both ends, a 5′ tail at both ends, or without any ss tail (see Fig. 5). These substrates were incubated with a reduced Srs2:DNA ratio at the lower reaction temperature of 23 °C. Under these conditions, although the substrate with the 3′ ss overhangs (*panel I*) was unwound by Srs2, neither the substrate with the 5′ tails (*panel II*) nor the blunt-end substrate (*panel III*) was acted upon efficiently. Specifically, after 2.5 min, while ~57% of the substrate containing 3′ overhangs had been dissociated (Fig. 5*A*, *panel I*, *lane 4* and Fig. 5*B*), <2% of the substrates with either 5′ ss overhangs (Fig. 5*A*, *panel II*, *lane 4* and Fig. 5*B*) or blunt ends (Fig. 5*A*, *panel III*, *lane 4* and Fig. 5*B*) had been unwound. Thus, a 5′ ssDNA tail is ineffective at stimulating the helicase activity of Srs2. The results are entirely consistent with the observed 3′ to 5′ polarity of Srs2 movement on ssDNA (16).

Minimal Length of 3′ Overhang for Srs2 Recruitment—Next, we examined the minimal amount of 3′ overhang required to target the Srs2 helicase to the DNA substrate. For this purpose, we prepared substrates that shared a common 40-bp duplex region and contained a 3′ ss tail of 2, 5, 8, 10, 12, or 16

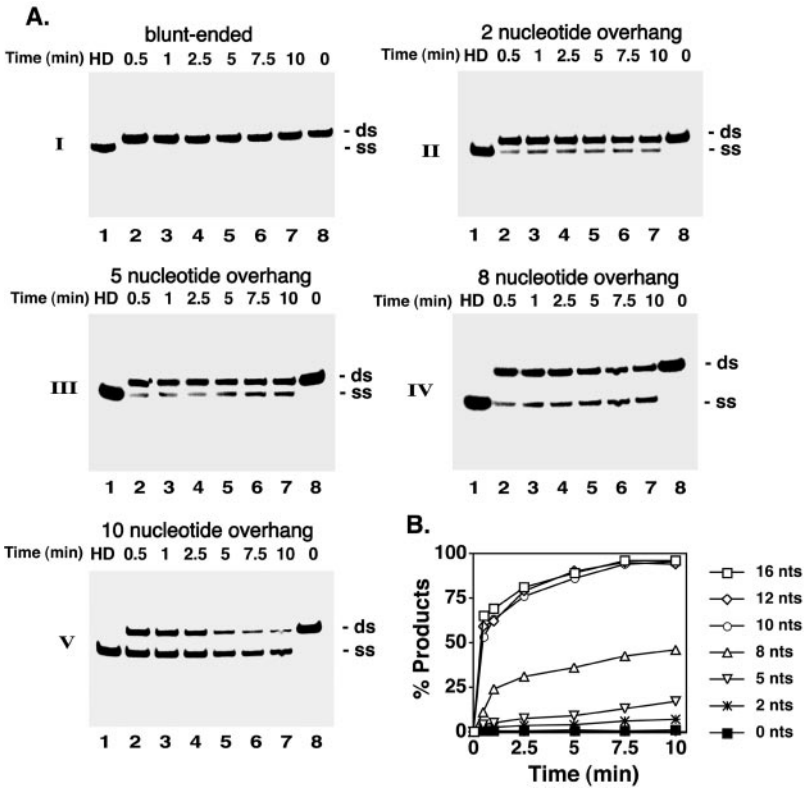

FIG. 6. **Effective length of 3′ ss tail for Srs2 targeting.** *A*, Srs2 (30 nM) was incubated for the indicated times at 23 °C with 40-bp DNA substrates (300 nM nucleotides) containing either blunt ends (*panel I*) or a 3′-ssDNA overhang of 2, 5, 8, or 10 nucleotides (*panels II*, *III*, *IV*, and *V*, respectively). In *lane 1*, the DNA substrate was dissociated by boiling for 1 min (*HD*); in *lane 8*, the substrate was incubated in buffer without Srs2 (*NP*). *B*, results from the reactions shown in *A* and from reactions containing substrates with 3′ overhangs of 12 and 16 nucleotides were plotted. *ds*, double strand; *nts*, nucleotides. All the experiments were repeated twice with very similar results.

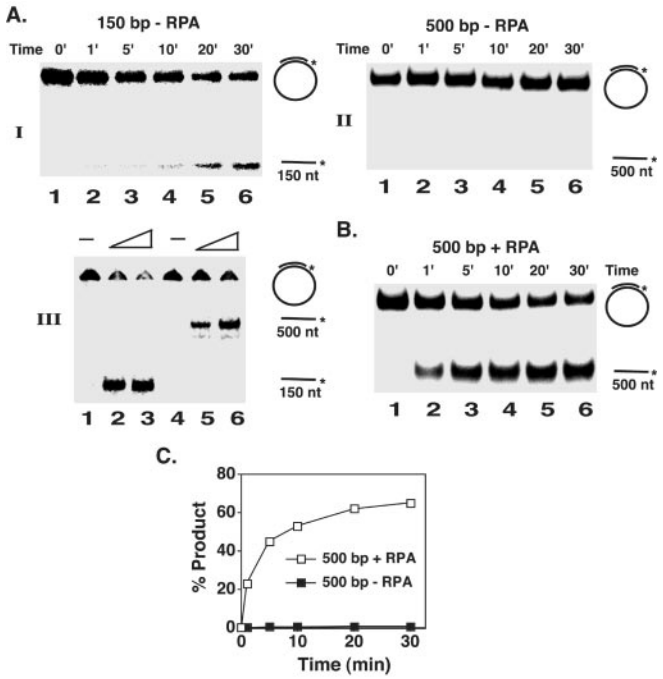

FIG. 7. **Enhancement of Srs2 helicase activity by RPA.** *A*, Srs2 (125 nM) was incubated at 30 °C with substrates containing 150-bp and 500-bp duplex regions (10 μM nucleotides, *panels I* and *II*) for the indicated times. The reactions were run in a 1.5% agarose gel, which was dried and analyzed in the PhosphorImager. In *panel III*, the substrates (1 μM nucleotides each) with 150-bp (*lanes 1–3*) or 500-bp (*lanes 4–6*) duplex region were incubated at 30 °C for 30 min with either 0.5 μM (*lanes 2* and *5*) or 1 μM Srs2 (*lanes 3* and *6*). In *lanes 1* and *4*, the DNA substrates were incubated in the absence of Srs2. The reaction mixtures were resolved in a 6% non-denaturing polyacrylamide gel and then analyzed in the PhosphorImager. *B*, Srs2 (125 nM) was incubated for the indicated times at 30 °C with the 500-bp partial duplex (10 μM nucleotides) in the presence of 0.5 μM RPA. Samples were analyzed as in *A*. *C*, the results from *panel II* of *A* and from *B* were plotted. *nt*, nucleotide. All the experiments were repeated twice with very similar results.

nucleotides. These substrates were incubated with Srs2 at 23 °C, and the level of substrate dissociation was determined in each case. The results from this series of experiments revealed that even a 2-nucleotide tail is capable of promoting DNA unwinding by Srs2 (Fig. 6*A*, *panels I* and *II*; Fig. 6*B*). Increasing the length of the 3′ ss overhang from 5 to 8 nucleotides resulted in a large increase in substrate unwinding (Fig. 6*A*, *panels III* and *IV*; Fig. 6*B*), with the near maximal level of unwinding being reached at 10 nucleotides (Fig. 6*A*, *panel V*; Fig. 6*B*). Thus, a 3′ ss overhang of about 10 nucleotides is needed for efficient targeting of Srs2 to the helicase substrate.

Srs2 Helicase Activity Is Enhanced by RPA—To assess whether the Srs2 helicase function could unwind longer DNA duplexes, we used two substrates that contained either a 150- or 500-bp region. These substrates were constructed by hybridizing radiolabeled DNA fragments obtained in a PCR reaction to ϕX174 viral (+) strand. As shown in Fig. 7*A*, *panel I*, Srs2 (125 nM) can dissociate the substrate with the 150-bp region (10 μM nucleotides) at 30 °C, but little, if any, unwinding of the substrate with the 500-bp duplex region (10 μM nucleotides) was seen under these conditions (Fig. 7*A*, *panels I* and *II*; Fig. 7*C*). At a much higher Srs2 concentration (1 μM) and with 10-fold less substrate (1 μM nucleotides), Srs2 can also efficiently unwind the 500-bp substrate (Fig. 7*A*, *panel III*).

One possible explanation for the above results (Fig. 7*A*) is that in unwinding long regions of duplex DNA, the once separated DNA strands reanneal. Such reannealing of DNA strands would effectively preclude the complete dissociation of long duplex regions, except when the helicase concentration is extremely high, such as in the experiment presented in Fig. 7*A*, *panel III*. Consistent with this postulate, the ability of a number of helicases to unwind longer substrates can be significantly enhanced by the inclusion in the DNA unwinding reaction of a single-strand binding protein, which sequesters ssDNA strands created as a result of unwinding to prevent their reannealing (22–24). When yeast RPA, a single-strand DNA-binding protein (25), was added with a low concentration of Srs2 (125 nM) to the 500-bp helicase substrate (10 μM nucleotides), the amount of displaced ssDNA product increased significantly (Fig. 7*B*). For instance, after only 5 min of incubation, ~40% of the 500-bp partial duplex has been unwound (Fig. 7B and C), as opposed to ≤1% substrate dissociation in the absence of RPA (Fig. 7*A*, *panel I*; Fig. 7*C*). We have found that *E. coli* single-strand binding protein (SSB) is just as effective as RPA in promoting the unwinding of the 500-bp substrate (data not shown).

DISCUSSION

In summary, we have shown that Srs2 protein has a highly robust ATPase activity that requires DNA, in particular ssDNA, for activation. In acting as a DNA helicase, Srs2 is specifically targeted to substrates that contain a 3′-ssDNA tail, and although we do not yet know the ssDNA binding site size for this protein, a minimum length of about 10 nucleotides is needed for its efficient targeting to helicase substrates. The fact that Srs2 prefers substrates with a 3′-ssDNA tail is congruent with a previous report by Rong and Klein (16), who deduced from their data that Srs2 translocates on ssDNA in the 3′ to 5′ direction. Because a free oligo dT molecule of 10 nucleotides is efficiently bound, as seen in experiments that examined the ATPase activity of Srs2, the apparent lack of an effect of a 40-nucleotide 5′ overhang in the DNA unwinding experiments suggests that Srs2 may simply slide off the ss tail because of its 3′ to 5′ direction of translocation on ssDNA (16). With a 3′ tailed DNA substrate, upon binding to the ssDNA region, we would expect Srs2 to translocate into the duplex region and hence produce a higher level of unwound product. We have shown that Srs2 by itself is not particularly adept at dissociating long duplex regions. Importantly, the unwinding of longer duplex substrates is enhanced by the addition of yeast RPA. Because *E. coli* SSB is similarly effective at promoting the unwinding of long DNA substrates, the stimulation afforded by RPA is likely because of its ability to sequester single-stranded DNA created by helicase action rather than to a specific interaction with Srs2. By sequestering single-stranded DNA, RPA would prevent the reannealing of separated DNA strands and could also help target Srs2 to the junction between ssDNA and the duplex region in the helicase substrates. Our results also reveal for the first time that under optimized conditions, Srs2 can efficiently unwind blunt-end DNA substrates.

Cells mutated for *SRS2* exhibit enhanced spontaneous and also DNA damage-induced mitotic recombination. In addition, combining the *srs2*Δ mutation with a null mutation in *SGS1*, which encodes a DNA helicase of the RecQ family, renders cells inviable (11, 26). Interestingly, the inviability of the *srs2*Δ *sgs1*Δ double mutant is fully rescued by deleting genes of the *RAD52* epistasis group (*e.g. RAD51, RAD52, RAD55*, etc.) required for homologous recombination, thus identifying inappropriate recombination as the underlying basis of cell inviability in this mutant (11, 13). It seems possible that in the *srs2*Δ *sgs1*Δ mutant, lesions that are normally processed by non-recombination-based repair pathways are now bound by recombination proteins, leading to the formation of nucleoprotein intermediates that cannot be resolved properly, thereby resulting in cell viability. The studies of Klein (13) have further

indicated that in combination with mutations in a variety of genes involved in DNA repair and replication, the *srs2* mutation causes a prolonged DNA damage checkpoint-mediated cell cycle arrest that can be overcome by crippling either the recombination machinery or the DNA damage checkpoint, further supporting the idea that Srs2 prevents the accumulation of aberrant DNA or nucleoprotein intermediates. From these genetic studies, it seems clear that Srs2 functions as an antagonist of homologous recombination under certain circumstances, and in this regard, can be viewed as an anti-recombinase.

It has been suggested that the Srs2 helicase activity is needed for reversing or dissociating cytotoxic DNA intermediates generated by the recombination machinery and, hence, is indispensable for the anti-recombinase function (12). The purification of Srs2 protein and the characterization of its ATPase and DNA helicase activities as presented here and elsewhere (16) should provide baseline information for the further pursuit of this hypothesis.

In recombination reactions that are initiated by a DNA double-strand break, the ends of the breaks are processed by a nuclease activity to yield ssDNA tails. The polymerization of the RecA-like recombinase Rad51 on these ssDNA tails leads to the formation of a nucleoprotein filament, often called the presynaptic filament (27, 28). The presynaptic filament recruits other recombination factors, including Rad54 and Rdh54 (20, 29, 30), and the higher order nucleoprotein complex that is assembled then mediates a search for a DNA homolog and the formation of DNA joints with the homolog. Interestingly, both we (17) and Fabre and coworkers (31) have recently found that Srs2 uses the free energy from ATP hydrolysis to dismantle the Rad51 presynaptic filament. Thus, the available results suggest that in its role as an anti-recombinase, Srs2 likely acts by means of turnover of Rad51 from bound ssDNA and by dissociating DNA intermediates made by the recombination machinery.

Recently, Aylon *et al.* (32) reported that *srs2* mutants have a diminished ability to repair a site-specific double-strand break. The authors showed that Srs2 functions in an early stage of break repair and suggested that Srs2 may be involved in facilitating the process of homology recognition or strand transfer carried out by Rad51 and associated factors. Whether the involvement of Srs2 in mediating double-strand break repair is related to its ability to displace inhibitory proteins from DNA and to unwind DNA remains to be established.

Vaze *et al.* (15) have found that *srs2* mutant cells are unable to recover or adapt from the DNA damage checkpoint-imposed G_2/M arrest. This abnormality of the *srs2* mutant can be effectively overcome by deleting *RAD51,* thus providing evidence that the persistence of Rad51-DNA nucleoprotein complexes leads to prolonged activation of the damage checkpoint machinery, even after the repair of damaged DNA has been completed. It is likely that the ability of Srs2 to dislodge Rad51 protein from DNA and to dissociate recombination DNA intermediates is critical for abolishing the signal that activates DNA damage checkpoint-mediated cell cycle arrest. In addition, it is possible that Srs2 evicts checkpoint-signaling complexes (*i.e.* the Mec1-Ddc2 and Rad17-Mec3-Ddc1 complexes) from DNA to attenuate the checkpoint responses (15).

In addition to its role in modulating recombination efficiency and promoting recovery from DNA damage checkpoint-imposed G_2/M arrest, Srs2 has also been implicated as a signaling molecule in the intra-S DNA damage checkpoint. Specifically, Liberi *et al.* (14) reported that in cells deleted for *SRS2*, the activation of the Rad53 kinase in response to DNA damaging treatment during S phase becomes partially impaired. It has been suggested that Srs2 generates or maintains a DNA structure needed for the activation of the intra-S checkpoint (14). It seems reasonable to propose that the DNA unwinding activity and the ability to evict bound proteins from DNA are germane for the checkpoint function of Srs2 as well.

REFERENCES

1. Wu, L., and Hickson, I. D. (2002) *Mutat. Res.* **509,** 35–47
2. Prakash, S., and Prakash, L. (2000) *Mutat. Res.* **451,** 13–24
3. Matson, S. W., Bean, D. W., and George J. W. (1994) *BioEssay* **16,** 13–22
4. Aboussekhra, A., Chanet, R., Zgaga, Z., Cassier-Chauvat, C., Heude, M., and Fabre, F. (1989) *Nucleic Acids Res.* **17,** 7211–7219
5. Lawrence, C. W., and Christensen, R. B. (1979) *J. Bacteriol.* **139,** 866–887
6. Schiestl, R. H., Prakash, S., and Prakash, L. (1990) *Genetics* **124,** 817–831
7. Aguilera, A., and Klein, H. L. (1988) *Genetics* **119,** 779–790
8. Rong, L., Palladino, F., Aguilera, A., and Klein, H. L. (1991) *Genetics* **127,** 75–85
9. Palladino, F., and Klein, H. L. (1992) *Genetics* **132,** 23–37
10. Klein, H. L. (2000) *Nat. Genet.* **25,** 132–134
11. Gangloff, S., Soustelle, C., and Fabre, F. (2000) *Nat. Genet.* **25,** 192–194
12. Schild, D. (1995) *Genetics* **140,** 115–127
13. Klein, H. L. (2001) *Genetics* **157,** 557–565
14. Liberi, G., Chiolo, I., Pellicioli, A., Lopes, M., Plevani, P., Muzi-Falconi, M., and Foiani, M. (2000) *EMBO J.* **19,** 5027–5038
15. Vaze, M. B., Pellicioli, A., Lee, S. E., Ira, G., Liberi, G., Arbel-Eden, A., Foiani, M., and Haber, J. E. (2002) *Mol. Cell* **10,** 373–385
16. Rong, L., and Klein, H. L. (1993) *J. Biol. Chem.* **268,** 1252–1259
17. Krejci, L., Van Komen, S., Li, Y., Villemain, J., Reddy, M. S., Klein, H., Ellenberger, T., and Sung, P. (2003) *Nature* **423,** 305–309
18. He, Z., Wong, J. M., Maniar, H. S., Brill, S. J., and Ingles, C. J. (1996) *J. Biol. Chem.* **271,** 28243–28249
19. Sung, P. (1997) *Genes Dev.* **11,** 1111–1121
20. Petukhova, G., Stratton, S., and Sung, P. (1998) *Nature* **393,** 91–94
21. Tsaneva, I. R., Muller, B., and West, S. C. (1993) *Proc. Natl. Acad. Sci. U. S. A.* **90,** 1315–1319
22. Harmon, F. G., and Kowalczykowski, S. C. (2001) *J. Biol. Chem.* **276,** 232–243
23. Matson, S. W., and George, J. W. (1987) *J. Biol. Chem.* **262,** 2066–2076
24. Nakagawa, T., Flores-Rozas, H., and Kolodner, R. D. (2001) *J. Biol. Chem.* **276,** 31487–31493
25. Wold, M. S. (1997) *Annu. Rev. Biochem.* **66,** 61–92
26. Lee, S. K., Johnson, R. E., Yu, S. L., Prakash, L., and Prakash, S. (1999) *Science* **286,** 2339–2342
27. Ogawa, T., Yu, X., Shinohara, A., and Egelman, E. H. (1993) *Science* **259,** 1896–1899
28. Sung, P., and Robberson, D. L. (1995) *Cell* **82,** 453–461
29. Petukhova, G., Sung, P., and Klein, H. (2000) *Genes Dev.* **14,** 2206–2215
30. Sung, P., Trujillo, K. M., and Van Komen, S. (2000) *Mutat. Res.* **451,** 257–275
31. Veaute, X., Jeusset, J., Soustelle, C., Kowalczykowski, S. C., Le Cam, E., and Fabre, F. (2003) *Nature* **423,** 309–312
32. Aylon, Y., Liefshitz, B., Bitan-Banin, G., and Kupiec, M. (2003) *Mol. Cell. Biol.* **23,** 1403–1417